

# RIGOROUS MODE-MATCHING METHOD FOR THE MODAL ANALYSIS OF THE T-JUNCTION CIRCULAR TO SIDE COUPLED RECTANGULAR WAVEGUIDE

Peter Krauss, and Fritz Arndt

Microwave Department, University of Bremen

P.O. Box 330 440

Kufsteiner Str., NW 1, D-28334, Bremen, Germany

**Abstract** - A rigorous field theoretical method is presented for the accurate modal analysis of the T-junction circular to sidecoupled rectangular waveguide which includes the so-called meniscus effect of the curved structure at the interface of the two different waveguide sections. The method is based on the mode-matching technique for the circular and rectangular waveguide portions of the structure in combination with the boundary-contour mode-matching (BCMM) principle for the intermediate waveguide section. In contrast to available approximate approaches, this method is rigorously valid also for large apertures, or for more than one aperture in the same plane, which are often required in typical filter, OMT or hybrid-T applications. The efficiency of the method is demonstrated by calculating a single T-junction with a large aperture and a double-aperture coupled T-junction. The theory is verified by excellent agreement with measurements.

## I. INTRODUCTION

THE T-JUNCTION circular to sidecoupled rectangular waveguide (Fig. 1) is an important waveguide key-building block for many applications such as multimode circular waveguide couplers [1], circular waveguide hybrid-T's [2], turnstile junctions [3], orthomode-transducers (OMT's) [3], and filters [4]. Up to now, such waveguide circuits were mostly designed experimentally [1] - [4].

Recently, some simplified field theoretical approaches for the analysis of the T-junction in Fig. 1 were reported which are valid for small coupling apertures: An integral equation technique in the spectral domain [5], and two mode-matching techniques, [6] - [7]. The implications in [5] and [6] are based on the adoption of two different surfaces (the cylindrical surface  $S_3$  (Fig. 1b) and the corresponding plane surface) to enforce the field continuity of the electric and

magnetic field. In [7], the cylindrical surface  $S_3$  is approximated by a linear relation. The rigorous inclusion of the so-called meniscus effect, i.e. the influence of the half-moon shaped section between the surface  $S_3$  (Fig. 1b) and the corresponding plane surface (through the points  $\varphi_u$  and  $\varphi_o$ , Fig. 1b), at the discontinuity between the circular and the sidecoupled rectangular waveguide, however, has turned out to be important for many usual applications of this T-junction structure, e.g. for hybrid-T or OMT purposes, where the influence of the full height aperture to sidecoupled standard rectangular waveguides has to be taken into account.

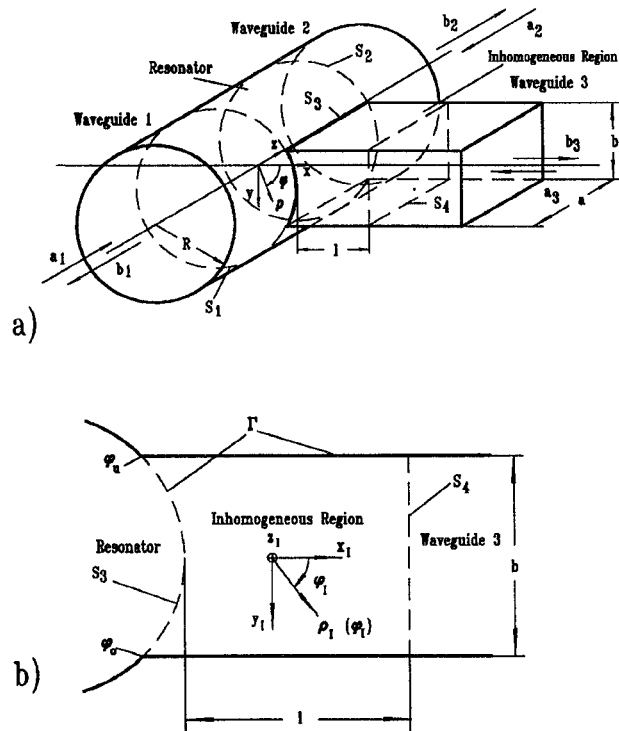


**Fig. 1:** T-junction circular to sidecoupled rectangular waveguide. (a) Designation of the ports and substructures. (b) Inhomogeneous intermediate region which is treated by the BCMM method.

The development of an efficient and accurate field theory based CAD method for this T-junction structure without any restrictions is therefore highly desirable. Moreover, this additional key-building block supplements the already available mode-matching tools [8], [9] significantly. The application of the generalized scattering matrix technique - together with the corresponding other mode-matching key-building blocks, e. g. the double step, iris, or rectangular T-junction discontinuities, [8], [9], - leads to the development of rigorous CAD programs for a comprehensive class of components, such as OMT's with multihole coupling sections [1], or side coupled circular cavity filters [4] with arbitrarily large apertures.

In this paper, we present a rigorous mode-matching method for the accurate modal analysis of the T-junction circular to sidecoupled rectangular waveguide, Fig. 1, which is based on the mode-matching technique for the circular and rectangular waveguide portions of the structure, in combination with the boundary-contour mode-matching principle [10] for the intermediate inhomogeneous waveguide section with the two different surfaces (Fig. 1b). In contrast to available approximate approaches, this method is valid also for large apertures, or even for more than one aperture in the same plane. The efficiency of the method is demonstrated by calculating a T-junction circular to an open sidecoupled standard  $WR-62$  waveguide, and a double-aperture coupled T-junction.

## II. THEORY

For the rigorous mode-matching treatment of the T-junction in Fig. 1, we separate the structure into six different subregions: Two one-sided short-circuited circular waveguide sections (designated in Fig. 1 with 'waveguide 1', 'waveguide 2'), a double-sided short-circuited circular waveguide section (designated in Fig. 1 with 'resonator'), the rectangular port waveguide 3, a region (designated with 'inhomogeneous region') of length  $l$  containing the half-moon shaped surface  $S_3$  at the discontinuity to the circular waveguide resonator, and (not explicitly indicated in Fig. 1) an infinitely thin artificial intermediate section at the common surface  $S_3$  within the angles  $\varphi_0$ ,  $\varphi_u$ , which allows the exact formulation of the boundary conditions at this interface.

Similar to [9] (for the rectangular T-junction), the resonator region in the circular waveguide T-junction (Fig. 1) consists of the superpositions of two circular waveguide sections waveguide 1 (which is open at

the plane  $z = -\frac{a}{2}$  and short-circuited at  $z = +\frac{a}{2}$ ) and waveguide 2 (which is open at the plane  $z = +\frac{a}{2}$  and short-circuited at  $z = -\frac{a}{2}$ ), and a cylindrical cavity region (which is short-circuited at both planes  $z = +\frac{a}{2}$  and  $z = -\frac{a}{2}$ ). The electromagnetic field in the circular waveguide sections 1 and 2 is derived from the corresponding expressions of the electric (e) and magnetic (h) vector potentials  $\psi$ :

$$\begin{aligned} \psi_{R_{1,2}}^e &= \sum_{m,n}^{\infty} J_m \left( \frac{x_{mn}}{R} \rho \right) \begin{pmatrix} \cos m\varphi \\ \sin m\varphi \end{pmatrix} \\ &\cdot \cos \left[ \beta_{R_{1/2,mn}}^e \left( z \mp \frac{a}{2} \right) \right] R_{1,2}^e, \end{aligned} \quad (1)$$

$$\begin{aligned} \psi_{R_{1,2}}^h &= \sum_{m,n}^{\infty} J_m \left( \frac{x'_{mn}}{R} \rho \right) \begin{pmatrix} \cos m\varphi \\ \sin m\varphi \end{pmatrix} \\ &\cdot \sin \left[ \beta_{R_{1/2,mn}}^h \left( z \mp \frac{a}{2} \right) \right] R_{1,2}^h, \end{aligned} \quad (2)$$

where  $x_{m,n}$  and  $x'_{m,n}$  are the zeros of the Bessel functions  $J_m$  and their derivatives  $J'_m$ , respectively, and  $R_{1,2}^{e,h}$  are the still unknown expansion coefficients.

In the cylindrical cavity region, the field is derived from the following expressions of the electric (e) and magnetic (h) vector potentials  $\psi$ :

$$\begin{aligned} \psi_{R_3}^e &= \sum_{m,p}^{\infty} J_m (k_{\rho_p} \rho) \begin{pmatrix} \cos m\varphi \\ \sin m\varphi \end{pmatrix} \\ &\cdot \cos \left[ \frac{p\pi}{a} \left( z + \frac{a}{2} \right) \right] R_3^e, \end{aligned} \quad (3)$$

$$\begin{aligned} \psi_{R_3}^h &= \sum_{m,p}^{\infty} J_m (k_{\rho_p} \rho) \begin{pmatrix} \cos m\varphi \\ \sin m\varphi \end{pmatrix} \\ &\cdot \sin \left[ \frac{p\pi}{a} \left( z + \frac{a}{2} \right) \right] R_3^h, \end{aligned} \quad (4)$$

with the coefficients  $R_3^{e,h}$ , and where the separation constant  $k_{\rho_p}$  is given by ( $k$  free space wavenumber)

$$k^2 = k_{\rho_p}^2 + \left( \frac{p\pi}{a} \right)^2. \quad (5)$$

The field in the 'inhomogeneous' region (Fig. 1b) is calculated rigorously by the boundary-contour mode-matching BCMM method [10] where the contour is described analogously to [10] by  $\Gamma = \rho(\varphi)$ . The electric and magnetic vector potentials  $\psi_4$  are expressed by the following complete set of functions:

$$\begin{aligned}\psi_{4z}^e &= \sum_{m,p}^{\infty} J_m(k_{\rho_p} \rho_4(\varphi_4)) \begin{pmatrix} \cos m\varphi_4 \\ \sin m\varphi_4 \end{pmatrix} \\ &\quad \cdot \cos \left[ \frac{p\pi}{a} \left( z_4 + \frac{a}{2} \right) \right] \alpha_4^e, \quad (6)\end{aligned}$$

$$\begin{aligned}\psi_{4z}^h &= \sum_{m,p}^{\infty} J_m(k_{\rho_p} \rho_4(\varphi_4)) \begin{pmatrix} \cos m\varphi_4 \\ \sin m\varphi_4 \end{pmatrix} \\ &\quad \cdot \sin \left[ \frac{p\pi}{a} \left( z_4 + \frac{a}{2} \right) \right] \alpha_4^h, \quad (7)\end{aligned}$$

with the separation constant

$$k^2 = k_{\rho_p}^2 + \left( \frac{p\pi}{a} \right)^2. \quad (8)$$

The boundary conditions on the boundary-contour  $\Gamma$  (Fig. 1b) of the inhomogeneous region and on the resonator cross-section are not inherently satisfied by the corresponding set of functions, equ. (3) - (8). Therefore, an infinitely thin artificial intermediate section along the surface  $S_3$  is introduced, where the modal electrical ( $\vec{e}$ ) and magnetic ( $\vec{h}$ ) field vectors are formulated by the following set of equations which assure the correct boundary conditions in  $\vec{u}_\varphi$  and  $\vec{u}_z$  direction:

$$\begin{aligned}\vec{e}_{pq} &= \left\{ \left[ \sin \left( \frac{p\pi}{a} \left( z + \frac{a}{2} \right) \right) \begin{pmatrix} \cos \left( \frac{q\pi}{\Delta\varphi} (\varphi - \varphi_u) \right) \\ \sin \left( \frac{q\pi}{\Delta\varphi} (\varphi - \varphi_u) \right) \end{pmatrix} \right] \right. \\ &\quad \left. \vec{u}_\varphi + \left[ \cos \left( \frac{p\pi}{a} \left( z + \frac{a}{2} \right) \right) \sin \left( \frac{q\pi}{\Delta\varphi} (\varphi - \varphi_u) \right) \right] \vec{u}_z \right\} A_{pq}, \\ \vec{h}_{pq} &= \left\{ \left[ \cos \left( \frac{p\pi}{a} \left( z + \frac{a}{2} \right) \right) \begin{pmatrix} \sin \left( \frac{q\pi}{\Delta\varphi} (\varphi - \varphi_u) \right) \\ \cos \left( \frac{q\pi}{\Delta\varphi} (\varphi - \varphi_u) \right) \end{pmatrix} \right] \right. \\ &\quad \left. \vec{u}_\varphi + \left[ \sin \left( \frac{p\pi}{a} \left( z + \frac{a}{2} \right) \right) \cos \left( \frac{q\pi}{\Delta\varphi} (\varphi - \varphi_u) \right) \right] \vec{u}_z \right\} B_{pq},\end{aligned}$$

where

$$\Delta\varphi = \varphi_0 - \varphi_u. \quad (9)$$

By matching the tangential field components at all boundaries, the still unknown expansion coefficients in all sections may be expressed in terms of the eigenmode amplitude expansion coefficients  $a_m, b_m$  (Fig. 1) of the circular and rectangular waveguide ports. Note that for the sections  $S_1, S_2, S_4$  the standard mode-matching technique may be applied. Rearranging of the equations yields the modal scattering matrix of the corresponding key-building block discontinuity, directly.

The modal scattering matrix of cascaded structures may be calculated by the known generalized scattering matrix technique [8], [9]. For all examples calculated in this paper, higher-order modes up to merely 80 GHz cut-off frequency (in the subsequent order of increasing cut-off frequency) are taken into account. The results are calculated by using a simple 486-level PC.

### III. RESULTS

In order to verify the presented rigorous mode-matching theory, a T-junction circular to sidecoupled rectangular waveguide with large aperture, i.e. the full rectangular waveguide cross-section, was fabricated, measured and compared with the calculations. Fig. 2 shows the scattering parameters of the T-junction with the following dimensions: Circular waveguide radius  $R = 6.985\text{mm}$ ,  $WR - 62$  rectangular waveguide ( $15.799\text{mm} \times 7.899\text{mm}$ ). Excellent agreement between theory and measurements may be stated.

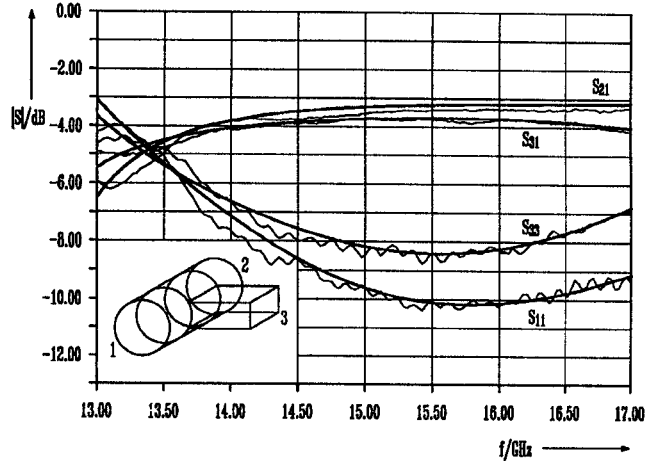


Fig. 2: Verification of the theory with measurements. T-junction circular waveguide (radius  $R = 6.985\text{mm}$ ) to sidecoupled open rectangular  $WR - 62$ -waveguide ( $15.799\text{mm} \times 7.899\text{mm}$ ). Scattering parameters as a function of frequency (thick lines: theory, thin lines: measurements).

In Fig. 3, it is demonstrated that the presented method is also well appropriate for a double aperture along the curved surface  $S_3$  (Fig. 1). The dimensions of the investigated T-junction structure are: Circular waveguide radius  $R = 13.208\text{mm}$ , aperture widths  $a = 10.160\text{mm}$ , aperture heights  $b = 2.540\text{mm}$ , smallest thickness of the aperture section  $t = 0.508\text{mm}$ ,

septum height  $h = 4.445\text{mm}$ , rectangular waveguide dimensions  $19.050\text{mm} \times 9.525\text{mm}$ . The scattering parameters in Fig. 3 are compared with calculations using an own FEM program. Excellent agreement is demonstrated.

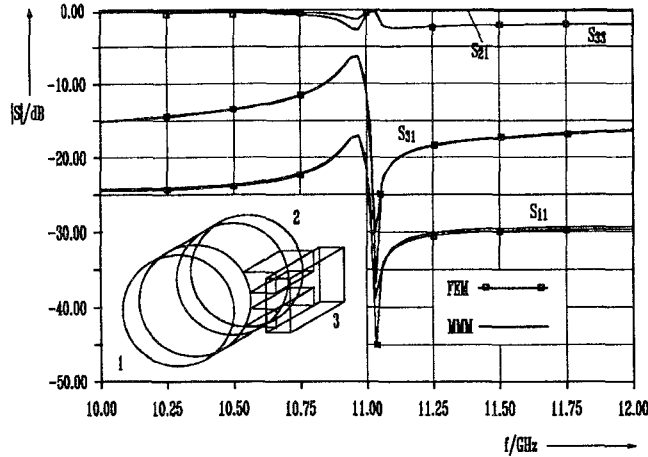


Fig. 3: T-junction circular to sidecoupled rectangular waveguide with a double aperture along the curved surface  $S_3$  (Fig. 1). Dimensions: Circular waveguide radius  $R = 13.208\text{mm}$ , aperture widths  $a = 10.160\text{mm}$ , aperture heights  $b = 2.540\text{mm}$ , smallest thickness of the aperture section  $t = 0.508\text{mm}$ , septum height  $h = 4.445\text{mm}$ , rectangular waveguide dimensions  $19.050\text{mm} \times 9.525\text{mm}$ . Scattering parameters in comparison with calculations using an own FEM program.

#### IV. CONCLUSION

A new, efficient and rigorous field theory method is proposed for the accurate analysis of the T-junction circular to sidecoupled rectangular waveguide including the hitherto neglected meniscus effect of the curved structure which has turned out to be important for the usual large apertures in standard OMT, hybrid and aperture coupled filter applications. The method is based on a combination of the flexible boundary-contour matching technique with the efficient mode-matching method. Therefore, only a modest number

of modes is required in order to ensure good convergence. The efficiency of the method is demonstrated at typical configurations for usual OMT or hybrid applications, where the full height aperture of the sidecoupled rectangular waveguide is required, and for filter applications, where often a double-aperture is used for the side coupling. The method is verified by measured results and results obtained by the finite element method which requires more computational effort. Because of the high numerical efficiency of the proposed method, merely a standard PC or a low-cost workstation is required for usual apertures.

#### References

- [1] A.C. BECK, "Measurement techniques for multimode waveguides", IEEE Trans. Microwave Theory Tech., vol. MTT-3, pp. 35 - 41, April 1955.
- [2] A.K. JAIN, and G.P. SRIVASTAVA, "A circular waveguide 'hybrid-T' and its applications", IEEE Trans. Microwave Theory Tech., vol. MTT-21, pp. 482 - 483, July 1973.
- [3] C.G. MONTGOMERY, R.H. DICKE, and E.M. PURCELL, "Principles of Microwave Circuits". New York: McGraw-Hill, 1948.
- [4] G.L. MATTHAEI, L. YOUNG, and E.M.T. JONES, "Microwave Filters, Impedance-Matching Networks and Coupling Structures". New York: McGraw-Hill, 1964.
- [5] A. MELLONI, M. POLITI, G.G. GENTILI, and G. MACCHIARELLA, "Field design of TE mode waveguide passband filters", in Proc. 22nd European Microwave Conf., Espoo, pp. 533 - 538, Aug. 1992.
- [6] G. F. CAZZATELLO, and V. DANIELE, "Electromagnetic model of circular-rectangular OMT", in Proc. 22nd European Microwave Conf., Espoo, pp. 557 - 560, Aug. 1992.
- [7] J. MARQUARDT, R. WENDEL, and M. GRIMM, "Calculation of the transition between a circular waveguide and a perpendicular rectangular waveguide", Frequenz, vol. 48, pp. 115 - 118, May 1994.
- [8] U. PAPZNER, and F. ARNDT, "Field theoretical computer-aided design of rectangular and circular iris coupled rectangular or circular waveguide cavity filters", IEEE Trans. Microwave Theory Tech., vol. MTT-14, pp. 462 - 713, March 1993.
- [9] T. SIEVERDING, and F. ARNDT, "Field theoretic CAD of open or aperture matched T-junction coupled rectangular waveguide structures", IEEE Trans. Microwave Theory Tech., vol. MTT-40, pp. 353 - 362, Feb 1992.
- [10] J.M. REITER, and F. ARNDT, "A boundary contour mode-matching method for the rigorous analysis of cascaded arbitrarily shaped H-plane discontinuities in rectangular waveguide", IEEE Microwave and Guided Wave Letters, vol. 2, pp. 403 - 405, Oct. 1992.